ADVANCED BIOSYSTEMS
www.adv-biosys.com

Proteomic and Metabolomic Characterization of Human Neurovascular Unit Cells in Response to Methamphetamine

Anna Herland, Ben M. Maoz, Edward A. FitzGerald, Thomas Grevesse, Charles Vidoudez, Sean P. Sheehy, Nikita Budnik, Stephanie Dauth, Robert Mannix, Bogdan Budnik, Kevin Kit Parker, and Donald E. Ingber**

The functional state of the neurovascular unit (NVU), composed of the blood–brain barrier and the perivasculature that forms a dynamic interface between the blood and the central nervous system (CNS), plays a central role in the control of brain homeostasis and is strongly affected by CNS drugs. Human primary brain microvascular endothelium, astrocyte, pericyte, and neural cell cultures are often used to study NVU barrier functions as well as drug transport and efficacy; however, the proteomic and metabolomic responses of these different cell types are not well characterized. Culturing each cell type separately, using deep coverage proteomic analysis and characterization of the secreted metabolome, as well as measurements of mitochondrial activity, the responses of these cells under baseline conditions and when exposed to the NVU-impairing stimulant methamphetamine (Meth) are analyzed. These studies define the previously unknown metabolic and proteomic profiles of human brain pericytes and lead to improved characterization of the phenotype of each of the NVU cell types as well as cell-specific metabolic and proteomic responses to Meth.

1. Introduction

The human neurovascular unit (NVU) that contains the blood–brain barrier (BBB) consists of brain microvascular endothelium, as well as perivascular pericytes, astrocytes, and neurons, plays a critical role in the metabolic homeostasis of the central nervous system (CNS), regulating drug accessibility to the brain, and protecting the brain from potentially harmful molecules found in the blood. Thus, it is important to understand how each of the individual cell types in the NVU responds to potentially harmful stimuli, such as drugs or toxins. While extensive brain cell-specific proteome mapping has been carried out recently in mice[1–3] these data do not directly translate to the human NVU as proteomic analysis of whole isolated vessels from human and mouse cortices demonstrated large

Prof. A. Herland, Dr. B. M. Maoz, E. A. FitzGerald, Dr. T. Grevesse, Dr. S. P. Sheehy, Dr. S. Dauth, Dr. R. Mannix, Prof. K. K. Parker, Prof. D. E. Ingber
Wyss Institute for Biologically Inspired Engineering at Harvard University
Boston, MA 02115, USA
E-mail: kkparker@seas.harvard.edu; don.ingber@wyss.harvard.edu

Prof. A. Herland
Division of Micro and Nanosystems
KTH Royal Institute of Technology
Stockholm 10044, Sweden

Prof. A. Herland
AIMES, Center for the Advancement of Integrated Engineering and Medical Sciences
Department of Neuroscience
Karolinska Institute
Stockholm 17177, Sweden

The ORCID identification number(s) for the author(s) of this article can be found under https://doi.org/10.1002/adbi.201900230.

DOI: 10.1002/adbi.201900230

Dr. B. M. Maoz, Dr. T. Grevesse, Dr. S. P. Sheehy, N. Budnik, Dr. S. Dauth, Prof. K. K. Parker
Disease Biophysics Group, Harvard John A. Paulson School of Engineering and Applied Sciences
Harvard University
Cambridge, MA 02138, USA

Dr. B. M. Maoz
Department of Biomedical Engineering
Faculty of Engineering
Tel Aviv University
Tel Aviv 6997801, Israel

Dr. B. M. Maoz
Department of Biomedical Engineering
Sagol School of Neuroscience
Tel Aviv University
Tel Aviv 6997801, Israel

Dr. C. Vidoudez
Small Molecule Mass Spectrometry Facility
Harvard University
Cambridge, MA 02138, USA

Dr. B. Budnik
Mass Spectrometry and Proteomics Resource Laboratory
Harvard University
Cambridge, MA 02138, USA

interspecies differences in expression of NVU-specific molecules, such as transporter proteins.[4] Transcriptional analysis of human primary brain microvascular endothelial cells has been carried out and again significant differences with that of mouse endothelial cells were noted.[5] Human brain pericytes have not been characterized at either the proteome or transcriptome levels; however, a recent mouse transcriptomics study led to the identification of potential new pericyte cell-specific markers.[1,6,7] Human astrocytes and neurons also have not been mapped with modern high-content proteomics, but transcriptome studies suggest several differences compared to mouse cells.[8]

We and others have recently reported the proteomic[9] and metabolomic[9,10] analysis of the individual compartments of a microfluidic human NVU-on-Chip (NVU Chip). In our previous work, the NVU Chip is composed of a 2-channel influx BBB Chip lined by human brain microvascular endothelial cells interfaced with human pericytes and astrocytes coupled via its perivascular channel to a Brain Chip containing human brain hippocampal stem cell-derived neuronal networks, which is further coupled to a second efflux BBB Chip again via its perivascular channel. In this on-chip configuration, the metabolic and proteomic characterization of the NVU cells was carried out of mixed populations of neurovascular cells that exhibited different phenotypes with or without fluidic coupling.[9] We have furthermore studied the contributions of the human brain microvascular endothelial cells interfaced with human pericytes and astrocytes to inflammatory processes in 2D cultures and 3D BBB Chip configuration.[11] While there is a need for advanced brain in vitro models,[12,13] the characterization of the metabolic and proteomic phenotypes of these individual NVU cell types in conventional cell cultures is still lacking, even though this format is far more widely applied for in vitro studies and high-throughput screening. Therefore, this study is based on data generated from separated conventional 2D cultures of each of the NVU cell types.

Several therapeutic and abusive drugs also have an impact on the NVU by altering the function of one or more of the cells that form the BBB.[14] Methamphetamine (Meth) is the second most abused drug in the US, with 13 million people 12 years of age or older having been reported to abuse the drug.[15,16] Regardless of the mode of administration, Meth is delivered to the brain through the circulating blood and it affects many NVU functions. For example, neuronal *N*-methyl-D-aspartate receptor receptors become overactivated due to Meth-mediated glutamate release, which leads to increased synthesis of superoxide and nitric oxide and eventually the formation of peroxynitrate, a major neurotoxin.[16] Exposure to Meth also triggers neuronal apoptosis through the p53 pathway,[17] and Meth-treated astrocytes and neurons reduce their glucose uptake due to inhibition of the glucose transporter protein-1.[18] Besides, Meth decreases tyrosine hydroxylase and tryptophan hydroxylase activities[19,20] and increases astrocytic expression of basic fibroblast growth factor and glial fibrillary acidic protein (GFAP) that are necessary for sensitization to amphetamine.[21] Lastly, Meth leads to metabolic alterations[22,23] and the degradation of the BBB,[14,24] triggering secondary injury to the neuronal cells. While the mechanism is still unclear,[24] Meth is known to affect BBB permeability[14,16,24] directly through inflammatory signaling that alters tight junctions and fluid-phase vesicular transport following glial activation, aminergic nerve damage, and hyperthermia, as well as by indirect mechanisms involving microglia activation and transmigrating leukocytes.[14] A more comprehensive picture cannot be described today because there is lack of detailed studies on the important structure–function relations of the primary human cells comprising the NVU, which will require high-resolution characterization of the proteome and secreted metabolome of the individual cell types.

Thus, here we set out to describe how the proteome of the individual NVU cell types correlates with their respective functionalities, and how it relates to the secreted metabolome of these cells under baseline conditions and when stressed by exposure to an acute dose of the recreational drug, Meth. We carried out the first proteomic and metabolomic (both targeted and untargeted) analysis of the four different primary human cell types that comprise the NVU analysis, in addition to measuring changes in respiration and cytokine responses in the presence and absence of Meth stimulation in these cell types. Importantly, we selected primary cells that are commercially available to allow for wide-spread applicability in basic research and drug development. We then related the important NVU functions (metabolic support, neurotransmitter uptake and synthesis, barrier function) to unique protein expression and secretome patterns for each cell type.

2. Results

2.1. Proteomic Characterization of Individual Primary Cell Types of the Human NVU

To characterize the unique properties of each cell type of the NVU, we separately cultured primary human microvascular endothelium, perivascular pericytes, astrocytes, or brain neural cells (derived from primary fetal neural hippocampal stem cells) in vitro, in wells. (**Figure 1**a,b). For each cell type, we characterized its morphology, proteome, and metabolome, as well as its cytokine and respiratory responses, in the presence or absence of Meth stimulation (Figure 1c). To maximize the usefulness of this data set in CNS research, we only used commercial suppliers of the cells in this study. Each cell type exhibited typical morphology and characteristic markers: the endothelial cells exhibited a cobblestone morphology and expressed zona occludens-1 (ZO1) along their apical borders (**Figure 2**a), the brain pericytes expressed platelet-derived growth factor-β (PDGFRβ) and Desmin, Phalliodin (Figure 2b and Figure S1, Supporting Information), and the astrocytes expressed GFAP (Figure 2c). We have previously demonstrated vascular endothelial cadherin in the endothelial cells and α-smooth muscle actin expression in the pericytes from the same vendor.[11] The neural stem cells differentiated to a mixed population of neural cells with characteristic morphology and extended outgrowth of cellular processes, quantified to ≈40% neuronal cells that stained for β-III-Tubulin and ≈60% GFAP-positive glial cells (Figure 2d).

Prof. D. E. Ingber
Vascular Biology Program and Department of Pathology
Boston Children's Hospital and Harvard Medical School
Boston, MA 02115, USA
Prof. D. E. Ingber
Harvard John A. Paulson School of Engineering and Applied Sciences
Harvard University
Cambridge, MA 02138, USA

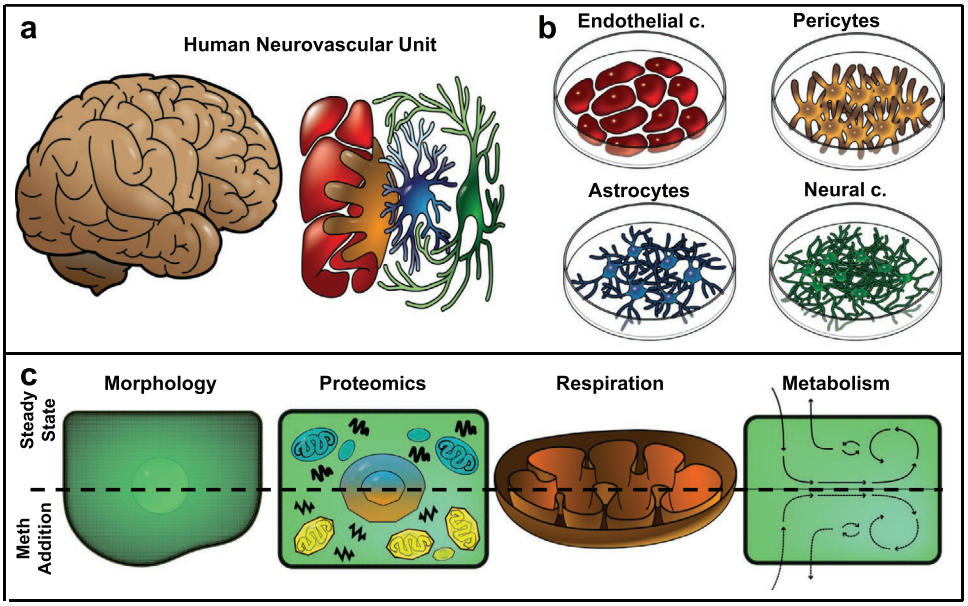

Figure 1. Characterizing the human neurovascular unit (NVU) in vitro. a) The human NVU is characterized by a tightly organized microvascular endothelium (red), perivascular pericytes (brown), astrocytes (blue), and brain neural cells (green), illustrated sketches of the human brain (left) and a part of a blood vessel (right). b) Human primary cells which make up the NVU were cultured in vitro independently of each other (the primary human neural cells were a mixture of primary neural stem cell-derived neurons and astrocytes). c) Comprehensive characterization was done for each of the cell types, which includes morphological, energetic, and cytokine assessments together with proteomics and metabolomics studies. The system was studied both at homeostasis and under stress due to methamphetamine (Meth) addition.

In addition to immunocytochemistry, untargeted mass spectrometry (m.s.) was used to characterize the cellular proteomes from whole cell lysates. We identified more than 2000 proteins in total with a large number of proteins that were unique for each cell type (Figure 2e). Endothelial cells showed the largest number of unique proteins (1405) compared to pericytes (771), astrocytes (904), and neural cells (811). In addition to these unique proteins, the common proteins between the different cell types were used to quantify the overlap and similarity between the cell types by measuring Pearson correlations. While the protein expression patterns of the endothelial cells and pericytes were highly correlated (0.82), the neural cultures exhibited the lowest correlation to all other cell types (0.63–0.64) (Figure 2f and Figure S2, Supporting Information). These findings are consistent with previous descriptions of the functional resemblance between endothelium and pericytes relative to neural cultures of murine cells.[25] We can further conclude the astrocytes' proteome was more similar to pericytes than either neural cells or endothelium. The pericyte proteomics moreover demonstrated expression of neuron-glial antigen-2 (also known as Chondroitin sulfate proteoglycan 4, CSPG4) which is a characteristic marker for this cell type.

To correlate protein mass abundance with their functionality (KEGG classification), we used proteomaps (Figure S3a,b and Movies S1–S4, Supporting Information), which showed that cytoskeletal proteins dominate the neural cell proteome whereas proteins relating translation and transcription are more dominant in the other three cell types. When we further analyzed the results using GOSlim to compare relative numbers of each of the significantly enriched protein, we can conclude that a small number of neural cytoskeletal proteins are dominating the pattern (Figure S2c, Supporting Information).

In addition, we used ingenuity pathway analysis (IPA)[56] to identify significant canonical pathways and their respective *z*-scores (Figure 2g) to estimate overall up- or downregulation of the pathways. The endothelial cells and pericytes had a relatively high Pearson correlation, but still displayed significant differences in terms of which pathways were dominant. Phosphoinositide 3-kinases (PI3K)/protein kinase B (AKT), extracellular signal-regulated kinases (ERK)/mitogen-activated protein kinases (MAPK), regulation of actin-based motility by Rho, actin nucleation, Signal transducer and activator of transcription 3 (STAT3), hepatocyte growth factor/scatter facto (HGF), and integrin signaling pathways were upregulated in pericytes compared to the endothelial cells, which is consistent with our observation that cultured pericytes were more proliferative and motile than the quiescent endothelial monolayer culture. The endothelium is the only cell type that exhibited upregulation of sphingosine-1-phosphate signaling, reinforcing the importance of this pathway for endothelial barrier function.[26] The primary astrocytes exhibited a low *z*-score for many of the pathways related to growth and motility (Figure 2g), which is consistent with the fact that we cultured these cells in serum-free medium. The high *z*-score for protein kinase A in the astrocytes is interesting since this pathway is critical for astrocyte responsiveness to the environment, both for neural support functions and inflammation.[14,27] The neural cells displayed a similar profile to the astrocytes with some exceptions, with more upregulated PI3K/AKT and neuregulin signaling and downregulated peroxisome proliferator-activated receptors (PPAR)/retinoid X receptor (RXR) and protein kinase A signaling, along with a total absence of expressed proteins in the Sphingosine-1-phosphate and ceramide signaling pathways.

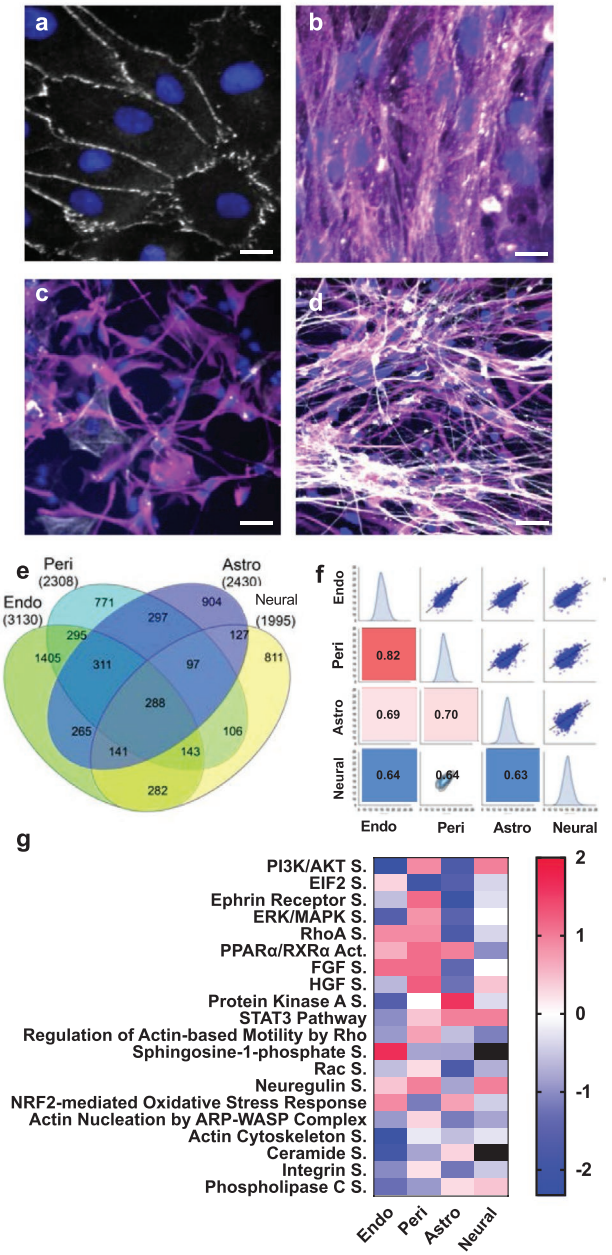

Figure 2. The similarity and discrepancy in the proteome of the cells in the human NVU. a–d) Immunocytochemistry of each cell type exhibiting characteristic markers, a) endothelial cells expressing zona occludens-1 (ZO-1, white), b) primary human brain pericytes or astrocytes that respectively expressed platelet derived growth factor-β (PDGFRβ, magenta), and c) glial fibrillary acidic protein (GFAP, magenta). F-actin labeled with phalloidin in gray. d) A mixed population of primary human neural cells (≈60% glial cells (GFAP, magenta) and 40% neurons (β-III-Tubulin, gray) (scale bars: a,b) 25 µm and c,d) 75 µm). e) Venn diagrams showing the overlap of the proteins that were found for each cell type. f) Pearson correlation of the label free quantification (LFQ values) quantifies the similarity in the protein profile between the different human NVU cell types, high correlation (red), and low correlation (blue), the table also presents the distribution of the samples. g) IPA was used to identify the canonical pathways and their regulation using Z-score (red, high Z-score, the pathway is upregulated and blue, low Z-score, the pathway is downregulated).

2.2. Effect of Meth on the NVU Cell Proteome, Cytokine Secretion, and Respiration

We then aimed for exposing the NVU cells to an acute single Meth dose that has the highest clinical relevance for CNS perivascular and parenchymal cells. Causal abuse of Meth results in plasma concentrations in the range 0.1×10^{-6}–11×10^{-6} M with up to ten times accumulation in brain tissue.[24] We exposed each of the NVU cell types to 50×10^{-6} M Meth for 24 h, a dose that did not produce any detectable effect on human endothelial barrier properties (Figure S4, Supporting Information) or morphological changes to any of the NVU cell types (Figure S5, Supporting Information). Noteworthy is that primary human brain microvascular cells in monoculture do not form strong a barrier, here we measured trans-endothelial resistance values of <25 Ω cm.[2] Meth administration resulted in a distinct change of protein expression patterns for each of the NVU cell types (**Figure 3** and Figures S2, S6, and S7 and Tables S1 and S2, Supporting Information). The cell type-specificity of these proteome-wide expression patterns was visualized using self-organizing maps created by gene expression dynamics inspector (GEDI) software based on changes in expression levels[28] (Figure 3a and Figure S6, Supporting Information). Meth exposure also changed the variability of the expression for each of the different cell types, as depicted by principal component analysis (PCA) (Figure 3b,c and Figures S6 and S7, Supporting Information). The neural cells primarily displayed an increase in the first PC compared to the other three cell types, which showed increased variability also in the second PC. In addition, the PCA showed that the proteins with the highest variability are associated with DNA maintenance, biosynthesis and folding, sorting, and degradation according to GOSlim biological process classification, which is consistent with previous studies.[14,29–31]

When IPA was used to identify the significant canonical pathways and their z scores (Figure 3d), the endothelial and neural cells were found to show strong upregulation in pathways related to inflammation (such as interleukin 8 (IL-8), high-mobility group protein 1 (HMGB1), and interferon regulatory factor (IRF)), proliferation, and migration (including FGF, integrin, PI3K/AKT, stress-activated protein kinases (SAPK)/jun amino-terminal kinases (JNK), and PDGF) upon Meth exposure. Astrocyte and pericytes, on the other hand, show no alternation or minor downregulations in the inflammation and migration pathways suggesting a lower degree of injury following acute Meth exposure.

As both our proteomic data and clinical observations indicate that inflammation is part of the brain's response to Meth,[14,16,32] we evaluated cytokines secreted by each cell type (data only shown for neural cells, **Figure 4**a,b). We found that at this level of Meth exposure, only the mixed neural cells exhibited significant increases in IL-6 (Figure 4a) and IL-8 (Figure 4b). In addition, we evaluated the respirational responses of these cells when exposed to Meth because it has been reported to induce mitochondrial damage.[33] Using a Seahorse assay, we compared the oxygen consumption rate (OCR) versus extracellular acidification rate (ECAR) as a measure of aerobic versus glycolytic respiration and the level of energy consumption (Figure 4c). As expected, these findings confirmed that the astrocytes are the most glycolytic cells, whereas the neural cells are the most energy demanding.[34]

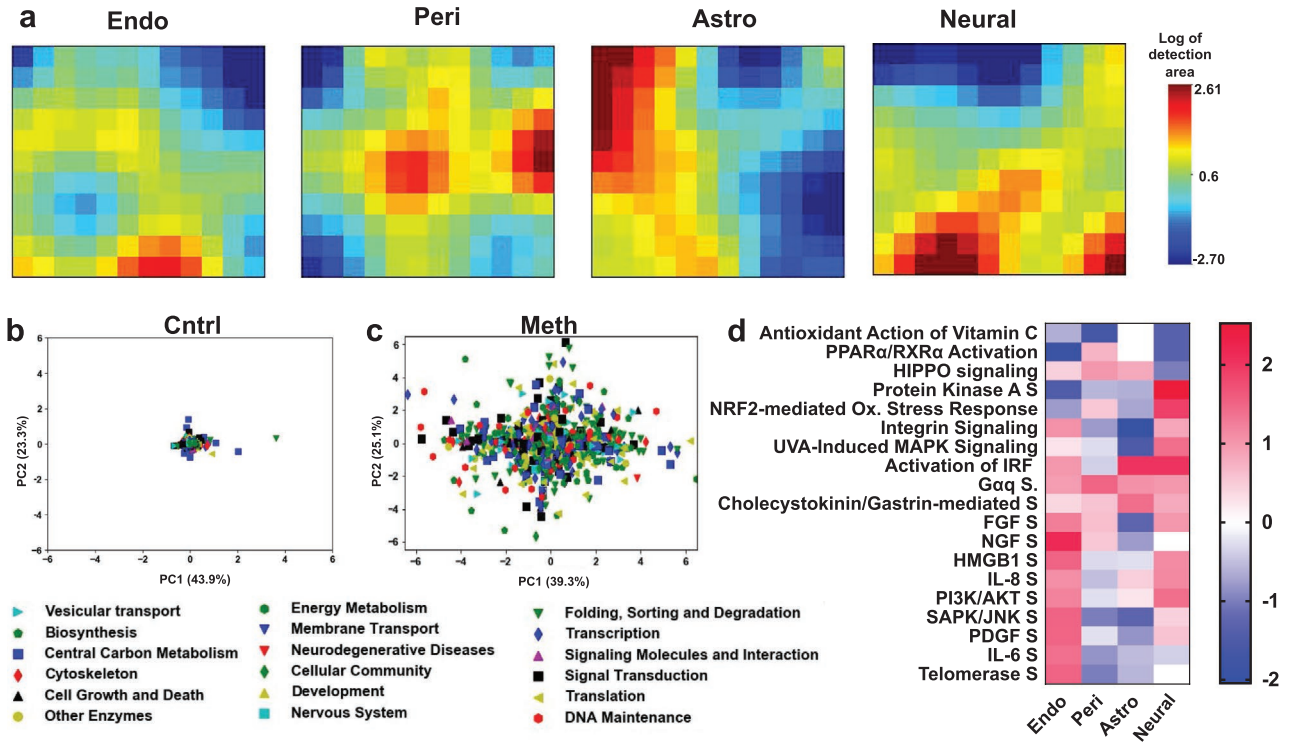

Figure 3. The impact of acute Meth challenge on the proteome of the cells in the human NVU. a) Protein expression was analyzed using gene dynamics inspector (GEDI). Differences in protein expression for Meth administration is displayed for each cell type visualizing low (or no) differences in blue, moderate differences in green/yellow, and high differences in red. Each sample is normalized to its untreated sample. The allocation map and the response normalized to "neural without Meth control" shown in Figure S4 in the Supporting Information. Principal component analysis (PCA) shows the variability in the protein expression all the NVU cells type, in b) homeostasis and c) under Meth administration shows the variance in the protein expression. For each protein, the biological function was assigned (legend at the bottom of (b) and (c)). d) IPA was used to identify the significant canonical pathways and their regulation which change due to Meth administration, using *Z*-score (red, high *Z*-score, the pathway is upregulated and blue, low *Z*-score, the pathway is downregulated).

Moreover, the endothelium is significantly more glycolytic compared to pericytes ($p < 0.0001$), almost comparable to astrocytes. Moreover, the endothelium is significantly less aerobic then pericytes and can be considered as displaying quiescent energy characteristics. These parameters have not been previously reported for pericytes, while the findings for the other cell types correlated well with previous experimental findings and with their known functionality in the NVU (e.g., the neural cells utilize high amounts of energy whereas the astrocytes must undergo high glycolysis to support the neurons).[34] In addition, we found that Meth exposure resulted in a significant change of the OCR/ECAR for the astrocytes, but not for the other cells (Figure 4c and Table S3, Supporting Information, $p = 0.0274$).

2.3. Targeted and Untargeted Metabolomic Analysis of NVU Cells

One of the most fundamental properties of the NVU is to control the supply of nutrients that are transported from the blood to the brain parenchyma, we, therefore, used both targeted and untargeted mass spectrometry and analyzed the cell culture supernatants for all small molecules (<550 Da) to identify the role of each cell type under baseline conditions and when exposed to Meth (**Figure 5**). Similar to the changes in protein expression we observed (Figures 2 and 3), each cell type exhibited a unique small molecular profile, which was identified via PCA of the untargeted mass spectrometry data (Figure 5a and Figure S8, Supporting Information). The cells did not change their PCA clustering in response to Meth administration, showing that the acute dose does not drastically change the metabolome of these cells. Moreover, while the neural cells and endothelium showed very distinct metabolomes, the pericytes and astrocytes displayed similar patterns much as we observed for their proteomes (Figure 2f), which suggests that pericytes might have an important role in the metabolic regulation in the NVU, similar to the astrocytes.

As a next step, we used Compound Discovery 2. Mummichog[35] and IPA (QIAGEN Inc.)[56] software to identify both metabolites and metabolic pathways that are associated with the small molecules that were identified with untargeted m.s. (Figure 5b,c and Table S5, Supporting Information). There were overlaps between the molecules that we identified within metabolic pathways using Compound Discovery 2.0 associated to KEGG, but each cell type also displayed a distinct set of secreted molecules (16 for endothelium, 5 for pericytes, 2 for astrocytes, and 13 for neural cells) (Figure 5b and Table S5, Supporting Information). The metabolic pathways that were significantly associated with the identified secreted molecules (Figure 5c) displayed a pattern similar to that detected by the

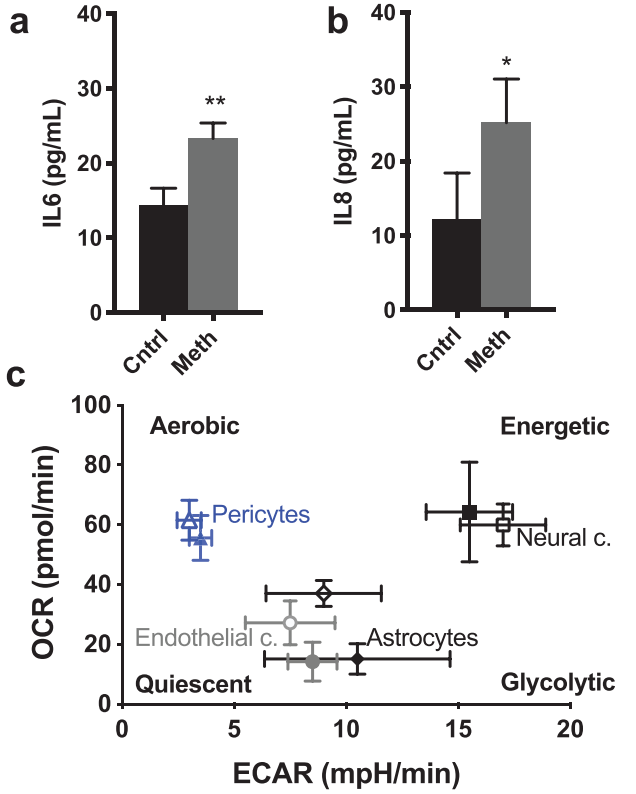

Figure 4. Inflammatory and respirational response upon Meth challenge on the human NVU cytokine release, IL6 a) **, $p = 0.0037$ and IL8 b) *, $p = 0.0292$ *t*-test, show significant response in neural cells, $n = 3$ and error bars showing standard deviation c) energy map for the cells that comprise the NVU, filled symbols are controls and open Meth treated cells. $n = 4$ and error bars are standard deviation. *p*-values for significant differences the cells within each treatment group (Control and Meth) are in Table S3 in the Supporting Information, a pairwise comparison with regular ANOVA and Sidak multiple comparison test for Control-Meth of each cell type for both ECAR and OCR.

PCA (Figure 5a), where the pericytes and astrocytes exhibited more similar patterns compared to endothelial and neural cells.

We then analyzed how Meth affects the metabolic pathways for each cell type. Interestingly, Meth administration reduced the number of the identified metabolic molecules produced by endothelial cells and astrocytes, whereas these numbers were increased in pericytes and neural cells (Figure 5c and Figures S8–S10 and Table S4, Supporting Information). Further characterization of the significant metabolic pathways (identified with IPA) revealed cell-type-specific responses to Meth. The overviewing observation is that endothelial cells, which are exposed to a very high dose by clinical comparisons show downregulation in all but Histamine and Biosynthesis. Neurons, astrocytes, and pericytes which are exposed to a Meth concentration often observed in the brain of abusers instead show upregulation in most of the metabolic pathways (Figure 5d). One specific pathway, glutathione synthesis, which is a significant pathway in the ROS (reactive oxygen species) regulation process, was downregulated in the endothelium and upregulated in the pericytes and astrocytes, whereas its level varied among the different neural cells (Figure 5d). This can be attributed to physiological function of astrocytes, where the astrocytes maintain brain homeostasis and protect neurons from ROS.[36] We then compared and contrasted the significant changes in protein expression and the secreted metabolome of the different human NVU cells that resulted from Meth exposure compared to baseline conditions (**Tables 1** and **2**). This revealed a significant correlation ($p < 0.05$) between the effects of Meth for proteomic and metabolomic pathways of isoenzymes nitric oxide synthases (iNOS) signaling, PI3K/AKT signaling, Stearate biosynthesis I, mitochondrial dysfunction, phagosome maturation, and transfer ribonucleic acid (tRNA) charging in all NVU cell types. In addition, there were correlations among a number of specific pathways in the proteomic and metabolomic analyses that significantly changed in two or more cell types (Table 1); of these, changes in citrulline and histamine have been recognized in methamphetamine studies previously.[29,31] As a metric of the difference between the NVU cell types, we identified Meth-induced changes in the proteome and metabolome that are unique to one of the cell types. The astrocytes presented the highest number of unique metabolic-proteomic correlated pathways which change due to Meth (7) followed by the endothelium (6), and neural cells (3), the pericytes did not show any unique metabolic-proteomic correlated pathways which change due to Meth. (Table 2). Interestingly, for each cell type, the unique metabolic-proteomic correlated pathways are associated to a specific biological process, for examples, the unique pathways that are observed in the endothelium are associated with urea production, astrocytes with glycine and neurons with nucleotide production.

To accurately quantify the glycolytic capacity of the NVU cells, and the impact of Meth exposure, we supplied the individual cell types with C13-labeled glucose and identified the related metabolites, lactate, pyruvate, glutamine, glutamate, and γaminobutyric acid (GABA) (Figure S11, Supporting Information) using targeted m.s. (**Figure 6**). We found that all of the cell types of the NVU carried out glycolysis, which is particularly interesting for the pericytes since this metabolic capacity was not described previously. The endothelium displayed the highest production of pyruvate (Figure 6a), lactate (Figure 6b) and glutamate (Figure 6c) compared to the other cell types. We also found that the astrocytes and neural cultures did not secrete detectable amount of glutamate (Figure 6d). While it is expected that neurons should secrete glutamate in the synaptic cleft, these studies revealed that the astrocytes (≈60% of the cells) in the culture take up the glutamate quickly (Figure 6c,d), as needed to avoid neurotoxicity.[34] Importantly, Meth administration significantly decreased pyruvate production by the endothelium which could directly affect the neuronal functionality, as pyruvate is discussed to be neuroprotective[37] (Figure 6 and Table S6, Supporting Information). Besides the nutrient source or metabolic pathways that produce the neurotransmitter, GABA, changed significantly in the neural cells exposed to Meth, which is a sign of altered neural function upon Meth stimulation (Figure 6e,f).

3. Discussion

In this study, we cultured separately each of the four human primary cell types that comprise the NVU and analyzed their

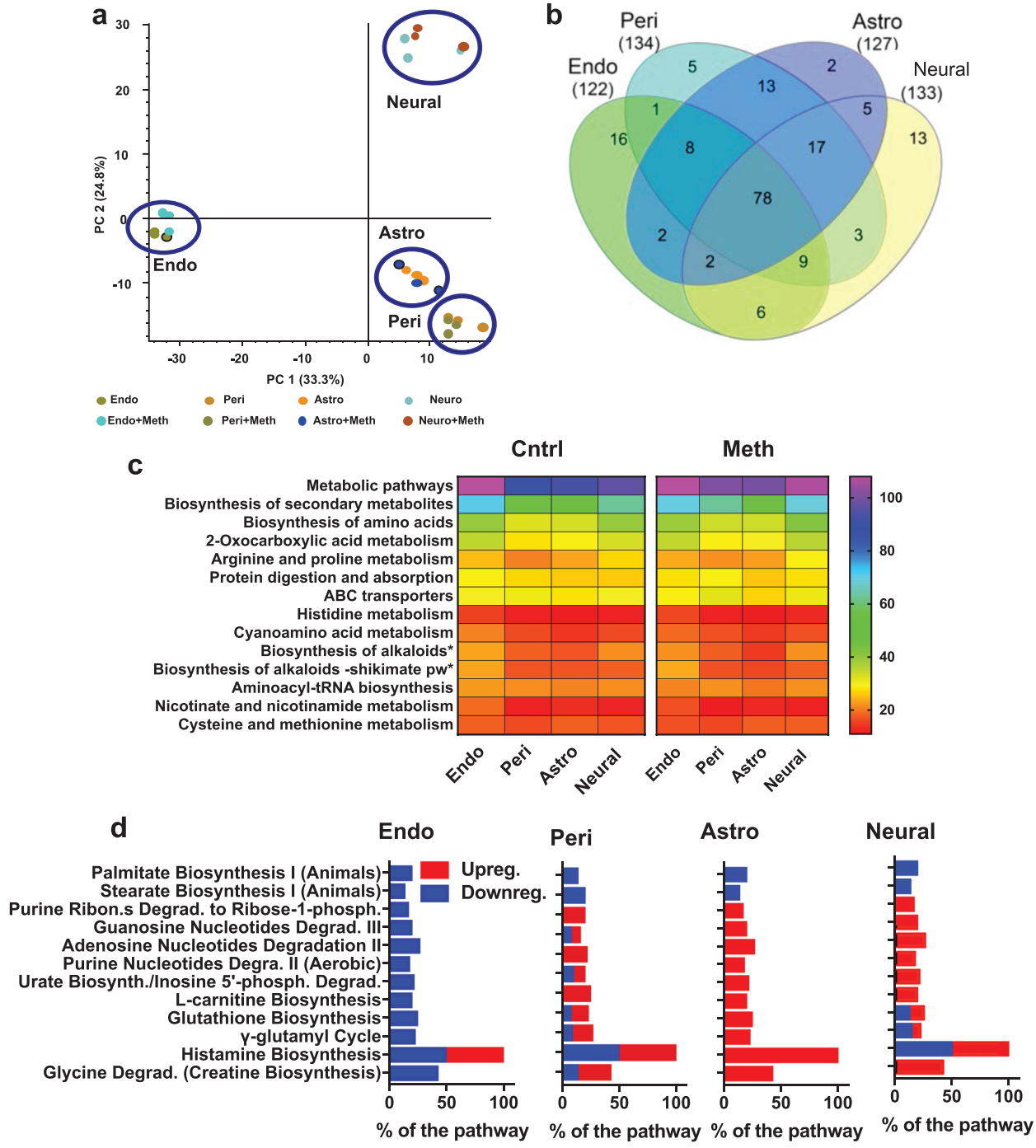

Figure 5. Untargeted metabolism of reveals in vivo like changes after acute Meth challenge on the human NVU. a) PCA was used to cluster and identify metabolic variance between each of the NVU cells, with and without Meth administration. Each cell type has a unique secretome. These differences are kept after Meth addition. b) Venn diagrams show the overlap in the metabolites that were found for each cell type. c) The number of molecular species in the secretome attributed to significant metabolic pathways that were identified with IPA for each of the NVU cells. In addition, a high number (≈150 of molecular species per cell) were attributed to other metabolic pathways. Each metabolite can be attributed to multiple pathways. The main metabolic pathways were identified in "Others" as shown in Figure S8 in the Supporting Information. d) Metabolic pathways identified with IPA which significantly change ($p < 0.05$) due to Meth challenge.

proteome and metabolome in the presence or absence of exposure to Meth. Importantly, this report is one of the first detailed proteomic and metabolomic characterizations of pericytes in vitro, which are the least characterized of the cells in the NVU even though their key contribution to NVU functionality is well established.[14,38] While proteomic analysis of human brain

Table 1. Correlated metabolic and proteomics pathways which are found in more than one of the NVU cell types.

Endo[a)]	Pericytes	Astrocytes	Neural
iNOS signaling	iNOS signaling	iNOS signaling	iNOS signaling
PI3K/AKT signaling	PI3K/AKT signaling	PI3K/AKT signaling	PI3K/AKT signaling
Stearate biosynthesis I (animals)	Stearate biosynthesis I (animals)	Stearate biosynthesis I (animals)	Stearate biosynthesis I (animals)
Mitochondrial dysfunction	Mitochondrial dysfunction	Mitochondrial dysfunction	Mitochondrial dysfunction
Phagosome maturation	Phagosome maturation	Phagosome maturation	Phagosome maturation
tRNA charging	tRNA charging	tRNA charging	tRNA charging
AMPK signaling		AMPK signaling	AMPK signaling
Palmitate biosynthesis I (animals)		Palmitate biosynthesis I (animals)	Palmitate biosynthesis I (animals)
Tryptophan degradation III (eukaryotic)	Tryptophan degradation III (eukaryotic)		Tryptophan degradation III (eukaryotic)
	Histamine degradation	Histamine degradation	Histamine degradation
Citrulline biosynthesis	Citrulline biosynthesis		
Mitochondrial L-carnitine shuttle pathway	Mitochondrial L-carnitine shuttle pathway	Mitochondrial L-carnitine shuttle pathway	
γ-glutamyl cycle		γ-glutamyl cycle	
eNOS signaling		eNOS signaling	
		Phenylalanine degradation IV (mammalian, via side chain)	Phenylalanine degradation IV (mammalian, via side chain)
		Putrescine degradation III	Putrescine degradation III

[a)]Canonical pathways which have significant change in both of their metabolic and proteomic expression. This table exhibits the correlation between the protein and metabolic expression, showing pathways are found in more than one of the NVU cell types.

microvessels has been carried out, the investigators were not able to distinguish contributions from endothelial cells from those due to closely interacting perivascular cells.[4] Human brain endothelial cell cultures have been characterized at the transcriptome level,[5] but not on the proteomic level. The same lack of proteomic characterization holds for human primary fetal astrocytes and primary stem cell-derived neural cells; however, there is an extensive transcriptomics study of human astrocytes from human adult and fetal tissue, which also includes some data on endothelial cells and neurons.[8] Our proteomic characterization of these four cell types that are all available from commercial sources should serve as a valuable reference for researchers setting up in vitro studies in conventional formats including high-through-put studies. The monoculture format is however not a physiological microenvironment and improved NVU phenotypes have been shown in many microfluid systems.[39,40] transepithelial electrical resistance (TEER) values of the brain endothelium is a prime example of this, here in monoculture we and others show values 20–100 Ω cm[2] whereas microfluidic systems have shown TEER ≈2000 Ω cm.[2,41] As a limitation in our approach, the cells that are commercially available are not isogenic. It is likewise important to emphasize that the neural cells are a mixed culture with neurons and astrocytes. The data presented in this manuscript demonstrates clearly that the mixed culture has a very different phenotype compared to the astrocyte monocultures.

Proteomic analysis of the endothelial cells and pericytes our morphological findings: the quiescent endothelial monolayer expressed proteins in pathways not associated with growth, whereas the motile and proliferating pericytes had their

Table 2. Correlated metabolic and proteomics pathways which are unique for each of the NVU cells.

Endo[a)]	Pericytes	Astrocytes	Neural
Glutathione biosynthesis		Glycine degradation (creatine biosynthesis)	L-carnitine biosynthesis
Urate biosynthesis/inosine 5'-phosphate degradation		Purine ribonucleosides degradation to ribose-1-phosphate	Purine nucleotides de novo biosynthesis II
CMP-*N*-acetylneuraminate biosynthesis I (eukaryotes)		Glycine biosynthesis I	Histidine degradation VI
Urea cycle		dTMP de novo biosynthesis	
Arginine biosynthesis IV		Superpathway of serine and glycine biosynthesis I	
Superpathway of citrulline metabolism		Glycine betaine degradation	
		Salvage pathways of pyrimidine ribonucleotides	

[a)]Canonical pathways which have significant change in both of their metabolic and proteomic expression. This table exhibits the correlation between the protein and metabolic expression. showing pathways that are unique to one of the NVU cells.

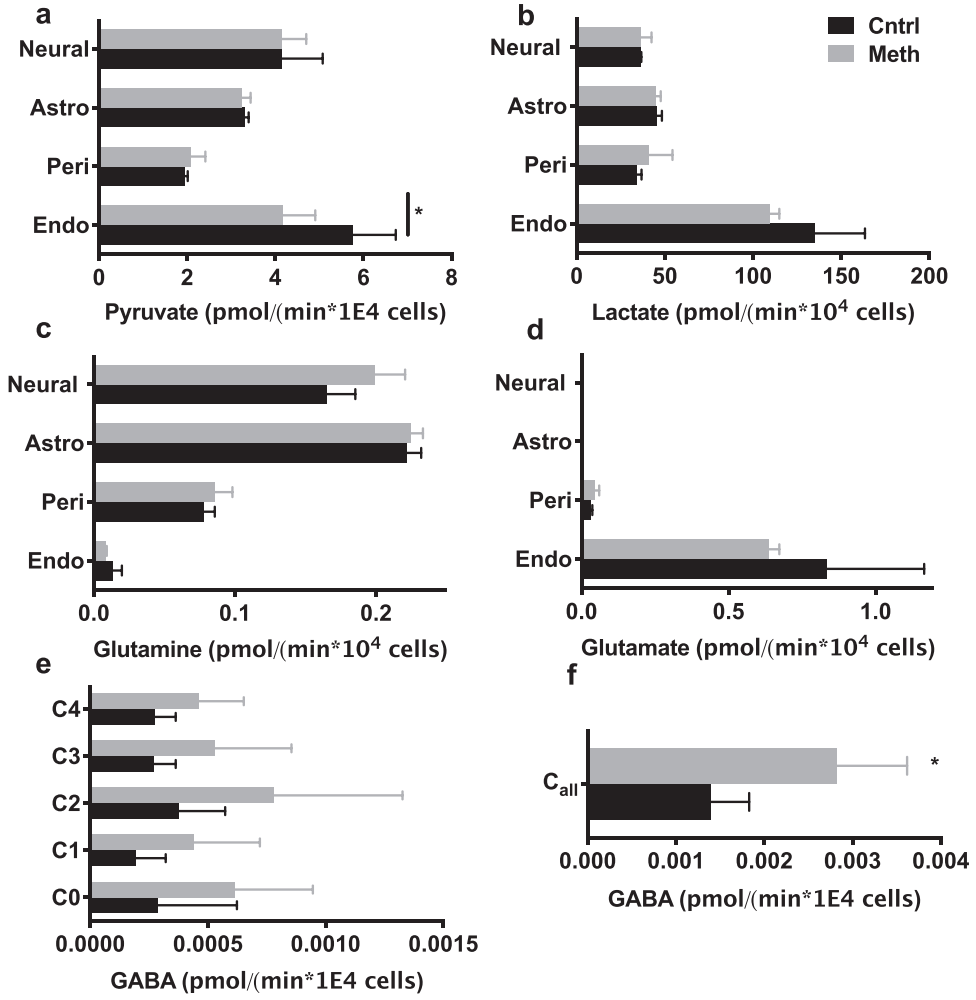

Figure 6. Targeted metabolism of labeled glucose reveals in vivo like changes after acute Meth challenge on the human NVU. The production rate of a) pyruvate, b) lactate, c) glutamate, d) glutamine, and e,f) GABA is presented for each cell type with (gray) and without (black) Meth. Endothelial cultures show the highest production rate of pyruvate, lactate, glutamate and are the most affected by Meth. As expected, the Astro and Neuro have the highest Glutamine rate, which is significantly affected by Meth addition. e,f) The synthesis of the GABA generates different numbers of labeled carbons; their distribution is not significantly affected by Meth addition. All data $n = 3$ and error bars showing the standard deviation. p-values for significant differences the cells within each treatment group (Control and Meth) are in Table S5 in the Supporting Information, a pairwise comparison with regular analysis of variance (ANOVA) and Sidak multiple comparison test for Control-Meth of each cell type for a) endothelial cells $p = 0.0197$ and t-test and f) $p = 0.0265$.

PI3K/AKT, ERK/MAPK, regulation of Actin-based Motility by Rho, actin nucleation, STAT3, HGF, and integrin signaling pathways upregulated. Like all primary cells, astrocytes are highly sensitive to culture conditions, especially the conventional use of proliferation-stimulating serum in the medium.[8] Here we cultured the cells at the lowest passage commercially available (P0) under serum-free conditions, and this is reflected in the dominant canonical pathways we observed in the astrocytes, which were consistent with a more quiescent phenotype. When comparing the proteomics of neural cells and astrocytes, it is important to consider that the primary human neural cells contain ≈60% astrocytes. When relating the proteomic data of the individual well to the NVU study[9] we can first conclude that the number of identified proteins in the comparably low cell number containing endothelial compartment (1679) and the perivascular compartment (1518) is lower than what can see from this larger plate culture, whereas the difference for the larger neuronal compartment (1970) is less. The more striking difference is the percentage of the proteins related to cytoskeletal processes which more dominant in the devices, probably indicating more dynamics in this environment compared to static wells.

The differences in respiration detected in the neurovascular cells allowed us to describe the relationship between oxidative phosphorylation (OCR) and glycolysis. As we also observed, endothelial cells have been demonstrated to rely on glycolysis,[42] which is surprising given the high oxygen concentration of blood compared to peripheral parenchymal tissue. Interestingly, the respiration properties of cultured pericytes, which to our knowledge have not been studied previously, were characterized by a much higher OCR/ECAR ratio than endothelial cells and astrocytes suggesting a higher degree of oxidative phosphorylation compared to glycolysis. Astrocytes were also observed to have a lower glycolytic phenotype than the neural cells which show a high energy oxidative phenotype.

The astrocyte population in the neural culture (60%) could be responsible for the upregulated glycolysis we observed to serve the high metabolic need of the neurons, a cell–cell interaction that has been demonstrated previously.[43] Overall, in our studies, the neural culture was the most energy demanding of the cultures.

In the untargeted metabolomics, we observed that the astrocytes and pericytes exhibited the most similar secretion patterns (Figure 5a) and number of secreted molecules that were exclusively common to these two cell types (Figure 5b). The targeted metabolomics showed that the endothelial cells secrete more lactate and exhibit the highest lactate/pyruvate ratio, which is interesting because the perivascular pericytes can use lactate as a substrate.[44,45] These results correlate to our previous work on a coupled NVU-Chip,[9] which identified that the vasculature secrete more lactate and pyruvate than the perivasculature. Pericytes have not previously been shown to synthesize glutamine and have been suggested to lack glutamine synthetase,[46] which is not consistent with our data since we can measure glutamine secretion. However, we must note that we cannot detect the protein glutamine synthetase in any of the NVU cells in the proteome. The absence of labeled glutamate in the media in the neural and astrocytes cultures suggests strong glutamate sequestering abilities of the astrocytes. These studies also confirmed that endothelial cells can produce glutamate[42] whereas pericytes only synthesize and secrete low levels of glutamate under these conditions. Overall, these results give a new insight into the pericyte metabolism, showing a lactate pyruvate ratio similar to astrocytes, very low glutamate secretion and glutamine secretion[47] and also supported by our previous work.[9] We observe that the endothelium is a major pyruvate producer. We relate these results to the previous findings that the brain vasculature and perivasculature has a significant contribution to the neural metabolism by providing it with essential metabolites, including pyruvate and lactate.

Meth abuse has many clinical manifestations, but here we focused only on the effects of 24 h exposure to Meth. Our dose of 50×10^{-6} M should be related to casual abuse of Meth results in plasma concentrations in the mid μM with up to ten times accumulation in brain tissue.[24] We aimed to compare cellular responses in the different NVU cell types after Meth exposure, we, therefore, chose a concentration that is moderate for the three perivascular and brain parenchymal cells, but which is high for the endothelial cells. Meth exposure has been shown to suppress the expression of tight junction proteins (ZO-1, occluding, and Claudin-5), and increase permeability in cultured brain microvascular endothelial cells[14,48,49] and mouse brain.[14,24,50,51] Oxidative stress and inflammatory signaling[14,24] (Cyclooxygenase-2 mediated) are also induced by Meth in cultured brain microvascular endothelial cells[52] as well as in rats.[24] The 24 h Meth dose did not produce visible morphology changes or induce any other stress signals in any of the cells (Figure S5, Supporting Information). We have shown that human primary brain endothelial cells under acute Meth dosing show a barrier breakdown with IC_{50} 1500×10^{-6} M (Figure S4, Supporting Information) and formation stress vacuoles at similar concentrations in previous studies.[9]

Changes in both proteomics and untargeted metabolomics show a differential response to Meth in the four human NVU cell types (Figures 3d and 5a). In the endothelial cells, Meth induces inflammatory pathways (e.g., IRF, IL6, IL8, HMGB1), and the upregulation of growth factor signaling pathways including PDGF signaling, which is consistent with studies that suggest Meth induces an injury and stress response at this dose[53] (Figure 3d). The endothelial NGF pathway upregulation could possibly mediated via PI3K/AKT upregulation to promote survival as previously demonstrated.[54,55] The Gαq pathway upregulation also can be linked to PI3K/AKT signaling and thereby promote migration and survival.[56] Lastly, the stress response in endothelial cells is manifested also in the stress induced SAPK/JNK pathway (Figures 3d and 5b,c)

Dysfunctional pericyte-endothelial interactions have been suggested to drive disease progression in neurodegenerative disease.[2] The effects of Meth on pericytes have only been reported in one in vitro study, which showed that Meth induces a pericyte migration response through stimulation of the sigma-1 receptor, with downstream activation of MAPK and PI3K/AKT pathways, demonstrated in a resulting increase of "P53 upregulated modulator of apoptosis" expression.[57] Our proteomic analysis revealed that the response of pericytes to Meth is different compared to the endothelial cells. The stress or injury response is less striking where none of the inflammatory pathways are activated, and also only two growth factor pathways (FGF and NGF) are upregulated. We observe a low upregulation of PPAR/RXR activation and nuclear transcription factor (NRF2)-mediated oxidative stress responses, combined upregulation of Gαq-signaling, and downregulation of PI3K/AKT signaling. Notably, previous observations for pathway PI3K/AKT was done in a pericyte cell line, which could affect the outcome.[57]

Astrocytes have been suggested to be activated by Meth, where the reactive phenotype was demonstrated by increased expression of GFAP.[58] Moreover, a very high dose (500×10^{-6} M) of repeated Meth dosing for 72 h resulted in cell cycle arrest, verified by quantitative polymerase chain reaction (qPCR) and fluorescence-activated cell sorting (FACS) analysis.[59] Here, with a more physiological, but short-term, dose of Meth, integrin, MAPK, IRF pathways increased in the astrocytes, these are also signatures of activation,[58,60] but we could not observe a significant change in GFAP expression with the untargeted proteomics.

The damages of Meth of neuronal cells have been extensively discussed in the literature, with a focus on the degradation of dopaminergic,[19,20,61,62] cholinergic[63] and serotonergic[64,65] neuronal functions. This has been modeled in rodents and is supported by clinical data from long-term abusers. Meth has also been shown to induce apoptosis in neurons[33] in vitro at high concentrations ($>250 \times 10^{-6}$ M) and in vivo.[33] Our study demonstrates a stress response similar to the patterns seen in the endothelial cells and upregulation of oxidative stress pathways affecting the neural cell population (Figure 3d). The activation of AKT/PI3K has previously been observed in neurons and suggested as a survival mechanism.[17] Our study with a mixed neural culture also verifies an inflammatory response by increased secretion of cytokines IL6 and IL8 (Figure 4a,b).

Metabolic changes have been observed in Meth abusers,[66] but no untargeted m.s. characterization has been attempted in human samples. For animal models, mouse[22] and rat[23] approaches have shown increased energy metabolism,

increased levels of excitatory amino acids and disruption of mitochondria and phospholipid pathways. Here we do not see a major shift in the PCA of metabolic profile (Figure 5a), which is consistent with in vivo animal studies.[22]

Treatment with Meth has decreased rat serum levels of lipids and free fatty acids.[23] In line with this (Figure 5d), the correlation between the metabolomics and proteomics, demonstrate downregulation of palmitate and stearate biosynthesis for all the NVU cell types. We also observe effects on L-carnitine pathway, a molecule that is involved in fatty acid metabolism. Interestingly, acetyl-L-carnitine has been used to protect neurons and astrocytes from adverse effects of Meth,[18] which indicates that an endogenous protective response in this pathway has been initiated. The regulation of several nucleoside degradation pathways (Figure 5d), is apparent, but varying over the cells, with downregulation only in endothelial cells. Upregulation of nucleoside degradation, as we observe in pericytes, astrocytes and neural cells could be a cellular compensation mechanism for energy depletion, as has been reported for other drugs and diseases[67] and discussed in the context of Meth.[18] The histamine biosynthesis pathway also shows a varying response, but with part of the pathway being upregulated in all the cells. This can be compared to observations of increased histamine levels in rats after acute Meth administration.[16,29] The regulation of glutathione and γ-glutamyl pathways, both associated with cellular redox processes support the discussion about Meth as an inducer of cellular stress. These findings correlate to rat in vivo studies, which confirmed alternations in glutathione levels after Meth dosing.[68] The targeted metabolomics also demonstrates minor changes after Meth treatment. The cellular stress signals (e.g., inflammatory pathways, growth factor signaling, glutathione and γ-glutamyl pathways) that were evident from the proteomics and untargeted metabolomics does not during our 24-hour dose manifest in increased lactate secretion levels, as previously seen in rats in vivo in a 5 d study.[23] We observed a decrease in pyruvate secretion in the endothelial cells, indicating an alternation in the energy metabolism of the cells. Furthermore, we detected an increased GABA secretion from the neural cultures. This correlated to previous studies in rat demonstrating how Meth increases both extracellular glutamate and dopamine, but also to increase GABA in regions of the brain (substantia nigra).[69] Here we observe a Meth induced increases of extracellular GABA in the neural cell culture.

Clinically meth-induced alternations of the brain have been mainly based on functional magnetic resonance imaging, positron emission tomography, and nuclear magnetic resonance for determination of volume changes of certain brain regional and certain specific metabolite levels and neurotransmitter localization.[70] Our study reveals effects in the proteome and metabolome on each NVU cell type separately, but still shows a high agreement with rat/mouse studies. This suggests that the separate NVU cells can be highly relevant as first preclinical assays for evaluation of drug effects on the BBB.

4. Conclusions

While the importance of the NVU is indubitable, there is a lack of knowledge on structure-function of each one of its components (endothelium, pericytes, astrocytes, and neural cells), both in homeostasis and under drug administration. In this work, we performed comprehensive proteomics and metabolomics analyses of each of the individual primary human cell types which comprise the NVU and analyzed their properties. We identified the metabolic and proteomic characteristics of human pericytes, which were not previously reported. Besides, the significant pathways as a response to Meth were identified and show that endothelial cells and neural cells show higher cellular stress compared to astrocytes and pericytes. This work presents new pathways that are active in the cells at homeostasis and as a response to Meth, which could be important when studying the CNS damage of Meth intoxication.

Supporting Information

Supporting Information is available from the Wiley Online Library or from the author.

Acknowledgements

A.H. and B.M.M. contributed equally to this work. This research was supported by the Wyss Institute for Biologically Inspired Engineering at Harvard University, Defense Advanced Research Projects Agency (DARPA) under Cooperative Agreement Number W911NF-12-2-0036 (D.E.I and K.K.P.); Wallenberg foundation, Grant 2015-0178, Forska Utan Djurforsok, and Carl Trygger Stiftelse, (A.H.); Azrieli Fundation and Brainboost (B.M.M.). The views and conclusions contained in this document are those of the authors and should not be interpreted as representing the official policies, either expressed or implied, of DARPA or the U.S. Government. The authors also thank T. Ferrante for technical assistance, M. Rosnach for artwork.

Conflict of Interest

D.E.I. is a founder and holds equity in Emulate, Inc. and chairs its scientific advisory board. K.K.P. is a consultant and a member of the scientific advisory board of Emulate, Inc.

Keywords

brain in vitro models, methamphetamine, neurovascular unit, primary cells

Received: September 20, 2019
Revised: July 2, 2020
Published online:

[1] M. Vanlandewijck, L. He, M. A. Mäe, J. Andrae, K. Ando, F. Del Gaudio, K. Nahar, T. Lebouvier, B. Laviña, L. Gouveia, Y. Sun, E. Raschperger, M. Räsänen, Y. Zarb, N. Mochizuki, A. Keller, U. Lendahl, C. Betsholtz, *Nature* **2018**, *554*, 475.
[2] Z. Zhao, A. R. Nelson, C. Betsholtz, B. V. Zlokovic, *Cell* **2015**, *163*, 1064.
[3] R. N. Munji, A. L. Soung, G. A. Weiner, F. Sohet, B. D. Semple, A. Trivedi, K. Gimlin, M. Kotoda, M. Korai, S. Aydin, A. Batugal,

A. C. Cabangcala, P. G. Schupp, M. C. Oldham, T. Hashimoto, L. J. Noble-Haeusslein, R. Daneman, *Nat. Neurosci.* **2019**, *22*, 1892.
[4] Y. Uchida, S. Ohtsuki, Y. Katsukura, C. Ikeda, T. Suzuki, J. Kamiie, T. Terasaki, *J. Neurochem.* **2011**, *117*, 333.
[5] E. Urich, S. E. Lazic, J. Molnos, I. Wells, P. O. Freskgard, *PLoS One* **2012**, *7*, e38149.
[6] L. He, M. Vanlandewijck, E. Raschperger, M. Andaloussi Mäe, B. Jung, T. Lebouvier, K. Ando, J. Hofmann, A. Keller, C. Betsholtz, *Sci. Rep.* **2016**, *6*, 35108.
[7] M. D. Sweeney, S. Ayyadurai, B. V. Zlokovic, *Nat. Neurosci.* **2016**, *19*, 771.
[8] Y. Zhang, S. A. Sloan, L. E. Clarke, C. Caneda, C. A. Plaza, P. D. Blumenthal, H. Vogel, G. K. Steinberg, M. S. Edwards, G. Li, J. A. Duncan3rd, S. H. Cheshier, L. M. Shuer, E. F. Chang, G. A. Grant, M. G. Gephart, B. A. Barres, *Neuron* **2016**, *89*, 37.
[9] B. M. Maoz, A. Herland, E. A. FitzGerald, T. Grevesse, C. Vidoudez, A. R. Pacheco, S. P. Sheehy, T. E. Park, S. Dauth, R. Mannix, N. Budnik, K. Shores, A. Cho, J. C. Nawroth, D. Segrè, B. Budnik, D. E. Ingber, K. K. Parker, *Nat. Biotechnol.* **2018**, *36*, 865.
[10] J. A. Brown, S. G. Codreanu, M. Shi, S. D. Sherrod, D. A. Markov, M. D. Neely, C. M. Britt, O. S. Hoilett, R. S. Reiserer, P. C. Samson, L. J. McCawley, D. J. Webb, A. B. Bowman, J. A. McLean, J. P. Wikswo, *J. Neuroinflammation* **2016**, *13*, 306.
[11] A. Herland, A. D. van der Meer, E. A. FitzGerald, T. E. Park, J. J. Sleeboom, D. E. Ingber, *PLoS One* **2016**, *11*, e0150360.
[12] P. Nikolakopoulou, R. Rauti, D. Voulgaris, I. Shlomy, M. B. Maoz, A. Herland, *Brain* **2020**, https://doi.org/10.1093/brain/awaa268.
[13] R. Rauti, N. Renous, B. M. Maoz, *Isr. J. Chem.* **2019**, *59*, https://onlinelibrary.wiley.com/doi/full/10.1002/ijch.201900052.
[14] R. K. Sajja, S. Rahman, L. Cucullo, *J. Cereb. Blood Flow Metab.* **2016**, *36*, 539.
[15] S. M. Kousik, T. C. Napier, P. M. Carvey, *Front. Pharmacol.* **2012**, *3*, 121.
[16] I. N. Krasnova, J. L. Cadet, *Brain Res. Rev.* **2009**, *60*, 379.
[17] T. F. Rau, A. Kothiwal, L. Zhang, S. Ulatowski, S. Jacobson, D. M. Brooks, F. Cardozo-Pelaez, M. Chopp, D. J. Poulsen, *Neuropharmacology* **2011**, *61*, 677.
[18] P. M. A. Muneer, S. Alikunju, A. M. Szlachetka, J. Haorah, *PLoS One* **2011**, *6*, e19258.
[19] A. J. Hotchkiss, J. W. Gibb, *J. Pharmacol. Exp. Ther.* **1980**, *214*, 257.
[20] H. C. Fibiger, E. G. McGeer, *Eur. J. Pharmacol.* **1971**, *16*, 176.
[21] A. N. Samaha, J. Stewart, *J. Neurosci.* **2000**, *20*, RC55.
[22] J. L. McClay, D. E. Adkins, S. A. Vunck, A. M. Batman, R. E. Vann, S. L. Clark, P. M. Beardsley, E. J. van den Oord, *Metabolomics* **2013**, *9*, 392.
[23] T. Zheng, L. Liu, J. Shi, X. Yu, W. Xiao, R. Sun, Y. Zhou, J. Aa, G. Wang, *Mol. BioSyst.* **2014**, *10*, 1968.
[24] P. Turowski, B. A. Kenny, *Front. Neurosci.* **2015**, *9*, 156.
[25] A. Armulik, G. Genové, C. Betsholtz, *Dev. Cell* **2011**, *21*, 193.
[26] B. A. Wilkerson, K. M. Argraves, *Biochim. Biophys. Acta, Mol. Cell Biol. Lipids* **2014**, *1841*, 1403.
[27] B. S. Huneycutt, E. N. Benveniste, *Adv. Neuroimmunol.* **1995**, *5*, 261.
[28] G. S. Eichler, S. Huang, D. E. Ingber, *Bioinformatics* **2003**, *19*, 2321.
[29] C. Ito, K. Onodera, E. Sakurai, M. Sato, T. Watanabe, *Brain Res.* **1996**, *734*, 98.
[30] J. J. Faure, S. M. Hattingh, D. J. Stein, W. M. Daniels, *Metab. Brain Dis.* **2009**, *24*, 685.
[31] J. L. Cadet, S. Jayanthi, M. T. Mccoy, M. Vawter, B. Ladenheim, *Synapse* **2001**, *41*, 40.
[32] N. A. Northrop, B. K. Yamamoto, *Front. Neurosci.* **2015**, *9*, 69.
[33] G. Stumm, J. Schlegel, T. Schäfer, C. Würz, H. D. Mennel, J. C. Krieg, H. Vedder, *FASEB J.* **1999**, *13*, 1065.
[34] P. J. Magistretti, I. Allaman, *Neuron* **2015**, *86*, 883.
[35] S. Li, Y. Park, S. Duraisingham, F. H. Strobel, N. Khan, Q. A. Soltow, D. P. Jones, B. Pulendran, *PLoS Comput. Biol.* **2013**, *9*, e1003123.
[36] M. Bélanger, I. Allaman, P. J. Magistretti, *Cell Metab.* **2011**, *14*, 724.
[37] Y. Zilberter, O. Gubkina, A. I. Ivanov, *Front. Neurosci.* **2015**, *9*, 17.
[38] A. Armulik, G. Genové, M. Mäe, M. H. Nisancioglu, E. Wallgard, C. Niaudet, L. He, J. Norlin, P. Lindblom, K. Strittmatter, B. R. Johansson, C. Betsholtz, *Nature* **2010**, *468*, 557.
[39] H. van Der, W. Marinke, *Tissue barriers* **2016**, *4*, e1142493.
[40] T. E. Park, N. Mustafaoglu, A. Herland, R. Hasselkus, R. Mannix, E. A. FitzGerald, R. Prantil-Baun, A. Watters, O. Henry, M. Benz, H. Sanchez, H. J. McCrea, L. C. Goumnerova, H. W. Song, S. P. Palecek, E. Shusta, D. E. Ingber, *Nat. Commun.* **2019**, *10*, 1.
[41] J. A. Brown, V. Pensabene, D. A. Markov, V. Allwardt, M. D. Neely, M. Shi, C. M. Britt, O. S. Hoilett, Q. Yang, B. M. Brewer, P. C. Samson, L. J. McCawley, J. M. May, D. J. Webb, D. Li, A. B. Bowman, R. S. Reiserer, J. P. Wikswo, *Biomicrofluidics* **2015**, *9*, 054124.
[42] D. Verdegem, S. Moens, P. Stapor, P. Carmeliet, *Cancer Metab.* **2014**, *2*, 19.
[43] C. N. Hall, M. C. Klein-Flügge, C. Howarth, D. Attwell, *J. Neurosci.* **2012**, *32*, 8940.
[44] C. Calì, A. Tauffenberger, P. Magistretti, *Front. Cell. Neurosci.* **2019**, *13*, 82.
[45] N. B. Hamilton, D. Attwell, C. N. Hall, *Front. Neuroenerg.* **2010**, *2*.
[46] M. D. Norenberg, A. Martinez-Hernandez, *Brain Res.* **1979**, *161*, 303.
[47] M. Kamouchi, T. Ago, T. Kitazono, *Cell. Mol. Neurobiol.* **2011**, *31*, 175.
[48] S. H. Ramirez, R. Potula, S. Fan, T. Eidem, A. Papugani, N. Reichenbach, H. Dykstra, B. B. Weksler, I. A. Romero, P. O. Couraud, Y. Persidsky, *J. Cereb. Blood Flow Metab.* **2009**, *29*, 1933.
[49] P. M. A. Muneer, S. Alikunju, A. M. Szlachetka, L. C. Murrin, J. Haorah, *Mol. Neurodegener.* **2011**, *6*, 23.
[50] T. Martins, S. Baptista, J. Gonçalves, E. Leal, N. Milhazes, F. Borges, C. F. Ribeiro, O. Quintela, E. Lendoiro, M. López-Rivadulla, A. F. Ambrósio, A. P. Silva, *Brain Res.* **2011**, *1411*, 28.
[51] N. A. Northrop, B. K. Yamamoto, *J. Neuroimmune Pharmacol.* **2012**, *7*, 951.
[52] P. S. Frankel, M. E. Alburges, L. Bush, G. R. Hanson, S. J. Kish, *Neuropharmacology* **2007**, *53*, 447.
[53] S. S. Oladipupo, C. Smith, A. Santeford, C. Park, A. Sene, L. A. Wiley, P. Osei-Owusu, J. Hsu, N. Zapata, F. Liu, R. Nakamura, K. J. Lavine, K. J. Blumer, K. Choi, R. S. Apte, D. M. Ornitz, *Proc. Natl. Acad. Sci. USA* **2014**, *111*, 13379.
[54] H. Kim, Q. Li, B. L. Hempstead, J. A. Madri, *J. Biol. Chem.* **2004**, *279*, 33538.
[55] M. J. Park, H. J. Kwak, H. C. Lee, D. H. Yoo, I. C. Park, M. S. Kim, S. H. Lee, C. H. Rhee, S. I. Hong, *J. Biol. Chem.* **2007**, *282*, 30485.
[56] IPA (QIAGEN Inc.), https://www.qiagenbioinformatics.com/products/ingenuitypathway-analysis.
[57] Y. Zhang, Y. Zhang, Y. Bai, J. Chao, G. Hu, X. Chen, H. Yao, *Exp. Cell Res.* **2017**, *356*, 28.
[58] Y. Zhang, X. Lv, Y. Bai, X. Zhu, X. Wu, J. Chao, M. Duan, S. Buch, L. Chen, H. Yao, *J. Neuroinflammation* **2015**, *12*, 29.
[59] A. R. Jackson, A. Shah, A. Kumar, *PLoS One* **2014**, *9*, e109603.
[60] I. N. Krasnova, B. Ladenheim, J. L. Cadet, *FASEB J.* **2005**, *19*, 1.
[61] S. J. O'Dell, F. B. Weihmuller, J. F. Marshall, *Brain Res.* **1991**, *564*, 256.
[62] M. A. Cervinski, J. D. Foster, R. A. Vaughan, *J. Biol. Chem.* **2005**, *280*, 40442.
[63] S. J. Kish, K. S. Kalasinsky, Y. Furukawa, M. Guttman, L. Ang, L. Li, V. Adams, G. Reiber, R. A. Anthony, W. Anderson, J. Smialek, L. DiStefano, *Mol. Psychiatry* **1999**, *4*, 26.

[64] D. E. Payer, E. L. Nurmi, S. A. Wilson, J. T. McCracken, E. D. London, *Transl. Psychiatry* **2012**, *2*, e80.
[65] Y. Liu, S. Brown, J. Shaikh, J. A. Fishback, R. R. Matsumoto, *Neuroreport* **2008**, *19*, 1407.
[66] C. C. Cruickshank, K. R. Dyer, *Addiction* **2009**, *104*, 1085.
[67] D. Boison, *Curr. Top. Med. Chem.* **2011**, *11*, 1068.
[68] O. Açikgöz, S. Gönenç, S. Gezer, B. M. Kayatekin, N. Uysal, I. Semin, A. Gure, *Neurotoxic. Res.* **2001**, *3*, 277.
[69] K. A. Mark, J. J. Soghomonian, B. K. Yamamoto, *J. Neurosci.* **2004**, *24*, 11449.
[70] L. Chang, D. Alicata, T. Ernst, N. Volkow, *Addiction* **2007**, *102*, 16.